APPLICATIONS OF ULTRASOUND TO MATERIALS CHEMISTRY

Kenneth S. Suslick

Department of Chemistry, University of Illinois at Urbana-Champaign, Urbana,
Illinois 61801; e-mail: ksuslick@uiuc.edu

Gareth J. Price

Department of Chemistry, University of Bath, Claverton Down, Bath BA2 7AY,
United Kingdom; e-mail: chsgjp@bath.ac.uk

ABSTRACT

The chemical effects of ultrasound derive primarily from acoustic cavitation.
Bubble collapse in liquids results in an enormous concentration of energy from
the conversion of the kinetic energy of the liquid motion into heating of the con-
tents of the bubble. The high local temperatures and pressures, combined with
extraordinarily rapid cooling, provide a unique means for driving chemical re-
actions under extreme conditions. A diverse set of applications of ultrasound to
enhance chemical reactivity has been explored with important uses in synthetic
materials chemistry. For example, the sonochemical decomposition of volatile
organometallic precursors in low-volatility solvents produces nanostructured ma-
terials in various forms with high catalytic activities. Nanostructured metals,
alloys, oxides, carbides and sulfides, nanometer colloids, and nanostructured
supported catalysts can all be prepared by this general route. Another important
application of sonochemistry in materials chemistry has been the preparation
of biomaterials, most notably protein microspheres. Such microspheres have a
wide range of biomedical applications, including their use in echo contrast agents
for sonography, magnetic resonance imaging, contrast enhancement, and oxygen
or drug delivery. Other applications include the modification of polymers and
polymer surfaces.

INTRODUCTION: ACOUSTIC CAVITATION

The study of chemical effects of ultrasound is a rapidly growing research area (1–7). Some of the most important recent aspects of sonochemistry have been its applications in the synthesis and modification of both organic and inorganic materials (8–12). High-intensity ultrasound can induce a wide range of chemical and physical consequences. The chemical effects of ultrasound fall into three areas: homogeneous sonochemistry of liquids, heterogeneous sonochemistry of liquid-liquid or liquid-solid systems, and sonocatalysis (which overlaps the first two). Applications of ultrasound to materials chemistry are found in all of these categories. Physical effects of high-intensity ultrasound, which often have chemical consequences, include enhanced mass transport, emulsification, bulk thermal heating, and a variety of effects on solids.

The chemical consequences of high-intensity ultrasound do not arise from an interaction of acoustic waves and matter at a molecular or atomic level. Instead, in liquids irradiated with high-intensity ultrasound, acoustic cavitation (the formation, growth, and collapse of bubbles) (13) provides the primary mechanism for sonochemical effects. During cavitation, bubble collapse produces intense local heating, high pressures, and very short lifetimes; these transient, localized hot spots drive high-energy chemical reactions. As described in detail elsewhere (4, 14–16), these hot spots have temperatures of $\sim 5000°C$, pressures of about 1000 atm, and heating and cooling rates above 10^{10} K/s. Thus, cavitation serves as a means of concentrating the diffuse energy of sound into a unique set of conditions to produce unusual materials from dissolved (and generally volatile) precursors. Chemical reactions are not generally seen in the ultrasonic irradiation of solids or solid-gas systems.

In addition, the interfacial region around cavitation bubbles has very large temperature, pressure, and (possibly) electric field gradients. Liquid motion in this vicinity also generates very large shear and strain gradients; these are caused by the very rapid streaming of solvent molecules around the cavitation bubble, as well as the intense shock waves emanated on collapse. These physical effects have special importance in polymer sonochemistry (described below).

Ultrasonic cavitation in liquid-solid systems also produces high-energy phenomena. The physical effects primarily responsible for such enhancements include (*a*) improvement of mass transport from turbulent mixing and acoustic streaming, (*b*) the generation of surface damage at liquid-solid interfaces by shock waves and microjets, (*c*) the generation of high-velocity interparticle collisions in slurries, and (*d*) the fragmentation of friable solids to increase surface area.

Cavitation near extended liquid-solid interfaces is very different from cavitation in pure liquids (13). Near a solid surface, bubble collapse becomes
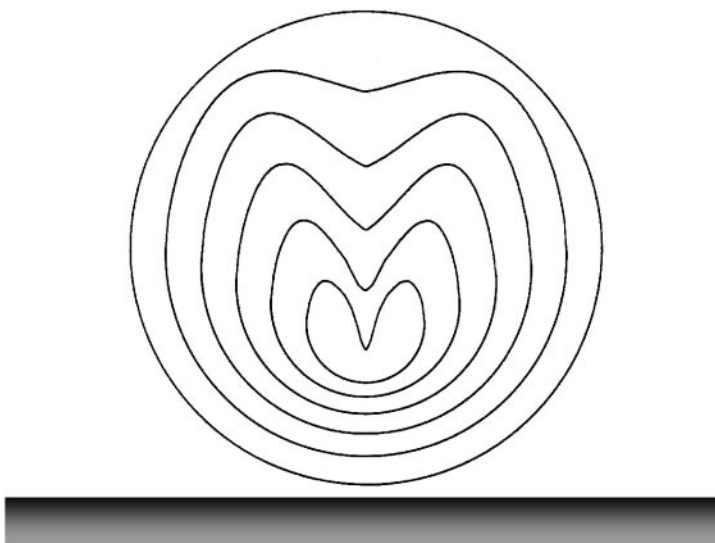
Figure 1   Formation of a liquid microjet during bubble collapse near an extended surface.

nonspherical, driving high-speed jets of liquid into the surface (Figure 1) and creating shockwave damage to the surface. Because most of the available energy is transferred to the accelerating jet, rather than the bubble wall itself, this jet can reach velocities of hundreds of meters per second. In addition, shockwaves created by cavity collapse in the liquid may also induce surface damage and the fragmentation of brittle materials. The impingement of microjets and shockwaves on the surface creates the localized erosion responsible for ultrasonic cleaning and many of the sonochemical effects on heterogeneous reactions. The importance of this process to corrosion and erosion phenomena of metals and machinery has been thoroughly reviewed elsewhere (17).

Finally, during ultrasonic irradiation of liquid-powder slurries, cavitation and the shockwaves it creates can accelerate solid particles to high velocities (18, 19). As discussed below, the interparticle collisions that result are capable of inducing striking changes in surface morphology, composition, and reactivity.

A wide range of commercial equipment is now readily available for sonochemical research. High-intensity ultrasonic probes (50 to 500 W/cm^2) of the type used for biological cell disruption are the most reliable and effective source for laboratory-scale sonochemistry and permit easy control over ambient temperature and atmosphere. Ultrasonic cleaning baths are less satisfactory, owing to their low intensities ($\approx$1 W/cm^2). For larger-scale irradiations, flow reactors

with high ultrasonic intensities are commercially available in 20-kW modular units (20).

Sonochemical rates for homogeneous reactions depend on a variety of experimental parameters such as vapor pressure of precursors, solvent vapor pressure, and ambient gas. To achieve high sonochemical yields, the precursors should be relatively volatile, because the primary sonochemical reaction site is the vapor inside the cavitating bubbles (21). In addition, however, the solvent vapor pressure should be low at the sonication temperature, because significant solvent vapor inside the bubble reduces the bubble collapse efficiency.

SONOCHEMICAL MODIFICATION OF MATERIALS

Effects of Ultrasound on Polymers

Although the search for new polymers with improved properties continues to attract great research interest, the economic drivers in the polymer industry demand continual improvement of existing materials. This has led to a large effort aimed at modifying existing polymers. For example, the interaction of an article with its surroundings is largely determined by its surface properties. The ability to alter the surface properties of an inexpensive commodity polymer is therefore of great economic interest. In a similar manner, modification of a bulk polymer by the incorporation of small amounts of other compounds is an economical method of producing highly functional materials. In addition, the material properties shown by a particular polymer sample depend critically on its molecular weight and chain microstructure so these must be precisely controlled. Sonochemistry has a part to play in each of these areas.

The effects of ultrasound on polymers can be both physical and chemical. Irradiation of liquids with ultrasound can cause solely physical changes from acoustic streaming, such as rapid mixing and bulk heating. Although cavitation is not always necessary for these effects, they almost always accompany cavitation. Examples of physical changes induced by ultrasound in polymer systems include the dispersal of fillers and other components into base polymers (as in the formulation of paints), the encapsulation of inorganic particles with polymers, modification of particle size in polymer powders, and, perhaps most important, the welding and cutting of thermoplastics (11). In contrast, chemical changes can also be created during ultrasonic irradiation, invariably as a result of cavitation, and these effects have been used to benefit many areas of polymer chemistry.

CHARACTERISTICS OF ULTRASONIC DEGRADATION   The degradation (meaning an irreversible lowering of the chain length caused by cleavage, and not necessarily any chemical change) of polymer chains in solution was one of the
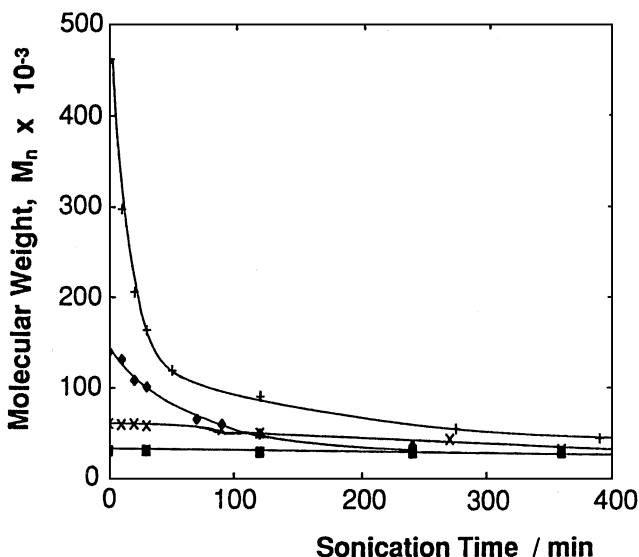
Figure 2 Ultrasonic degradation of 1% solutions of narrow polydispersity polystyrenes in toluene (11).

first reported effects of high-intensity ultrasound (22, 23). Although the precise origin is still open to debate, the process is now understood in sufficient detail to make it commercially applicable in a number of areas (24, 25). The basic effects (26) of irradiating a polymer solution with power ultrasound are shown in Figure 2, with polystyrene in toluene as an example.

The degradation proceeds more rapidly at higher molecular weights and approaches a limiting value, M_{lim}, below which no further degradation takes place (in this case $\sim$30,000). Polymers with this value or lower values are unaffected by ultrasound under these conditions. These effects have been reported in all types of macromolecules in solution and include both organic (22, 23) and inorganic [e.g. poly(organosiloxanes) and polyorganosilanes (27)] polymers in organic solvents and various polymers in aqueous media [such as polyethylene oxide (28), cellulose (29), polypeptides, proteins (30), and DNA (31)]. This common behavior is a result of a physical process that is independent of the chemical nature of the polymer, but rather depends on the polymer chain dimensions in solution. A large number of studies have demonstrated that the rate of degradation and M_{lim} are insensitive to the nature of the polymer when sonicated under the same conditions. Encina et al (32) found that the rate of degradation of poly(vinyl pyrrolidone) increased tenfold when the polymer was prepared with a small number of peroxide linkages in the backbone, suggesting

that chain cleavage can occur preferentially at weak spots in the chain. It is clear, however, that there must be a substantial difference in the relative bond energies for this effect to be noticed.

Many studies have been performed to characterize the rate of degradation in order to develop quantitative models of the process. In summary, the degradation proceeds faster and to lower molecular weights at lower temperatures, in more dilute solutions, and in solvents with low volatility. This pattern follows the effect of the parameters on cavitational bubble collapse. Sonication at higher temperatures or in volatile solvents results in more vapor entering the bubble and so cushioning the collapse, making it less violent. In dilute solutions, the polymer chains are not entangled and so are free to move in the flow fields around the bubbles. As expected, the degradation is more efficient at high ultrasonic intensities, owing to the greater number of bubbles with larger radii. Many other factors have been quantified, including the nature of any dissolved gases and the conformation that the polymer adopts in solution. Hence, by suitable manipulation of the experimental conditions, one can exert a great deal of control over the degradation process.

Although there is still some debate about the precise origins of the degradation, it has been shown that under conditions that suppress cavitation, degradation does not occur. The polymer chains are subjected to extremely large forces in the rapid liquid flows near collapsing cavitation bubbles and in the shock waves generated after bubble implosion; these can result in the breakage of a bond in the chain. There is no evidence that the extreme conditions of temperature found in cavitation bubbles contribute to polymer degradation in nonaqueous liquids, because the polymer chains have negligible vapor pressure and are unlikely to be found at the bubble interface. In contrast, however, pyrolysis can occur in aqueous solutions in which hydrophobic polymers concentrate at the bubble-air interface.

The kinetics and regiospecificity of ultrasonic degradation are different from those of thermal processes. Thermal degradation produces cleavage at random points along the chain, whereas ultrasonic degradation is much more specific, with cleavage occurring preferentially near the middle of the chain (33). The most quantitative model for this comes from the work of Van der Hoff & Gall (34), who investigated the degradation of polystyrene in tetrahydrofuran. They found that the degradation could be best modeled when it was assumed that the probability of chain breakage was distributed in a Gaussian manner within ~15% of the center of the chain. This center cleavage model is also consistent with the stretching and breakage mechanism suggested above. Degradation in shear fields of capillary flow (35) or in high-shear stirrers (36) also results in preferential breakage at the chain centers. A comparison of the chain breakage caused by ultrasound and extensional flows was published recently (37).
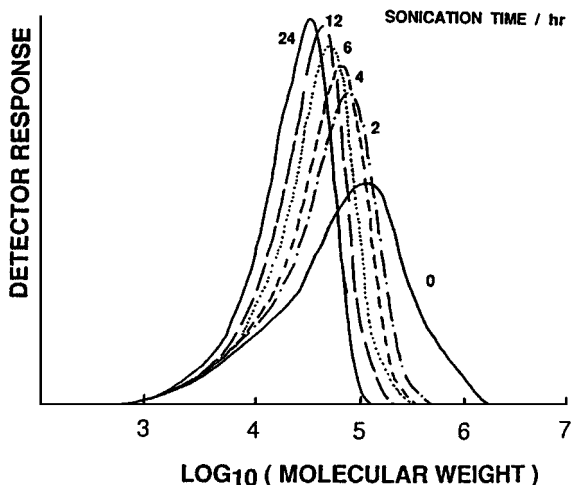
Figure 3 Gel permeation chromatography chromatograms of a 2% solution of a polyalkane sonicated in toluene (11); the numbers by each curve indicate the duration of sonication in hours.

APPLICATIONS OF ULTRASONIC DEGRADATION   The molecular-weight dependence of the degradation means that longer chains are preferentially removed from a sample and the polydispersity of the polymer is changed. Thus, degradation can be used as an additional processing parameter to control the molecular-weight distribution. For example, Figure 3 shows gel permeation chromatography (GPC) chromatograms of a polymer solution undergoing sonication (GJ Price, unpublished data). The degradation of the higher-molecular-weight species narrows the distribution markedly, and after 24 h of sonication, no material with molecular weight >100,000 remains. A recent commercial process, in fact, uses a sonochemical treatment during the final processing stage to control the molecular-weight distribution to give the desired processing properties of the polymer (11).

In all the carbon backbone polymers studied to date, the primary products of the degradation are radical species arising from homolytic bond breakage along the chain. The evidence for macromolecular radicals arises from radical trapping experiments as well as from the use of electron spin resonance spectroscopy (39). A second application of the degradation uses these macromolecular radicals as initiating species in the preparation of copolymers. A number of workers have sonicated mixtures of two polymers dissolved in a common solvent. Combination of the two different macromolecule fragments leads to formation of a block copolymer. However, this can be difficult to separate from the starting materials, and there are problems in
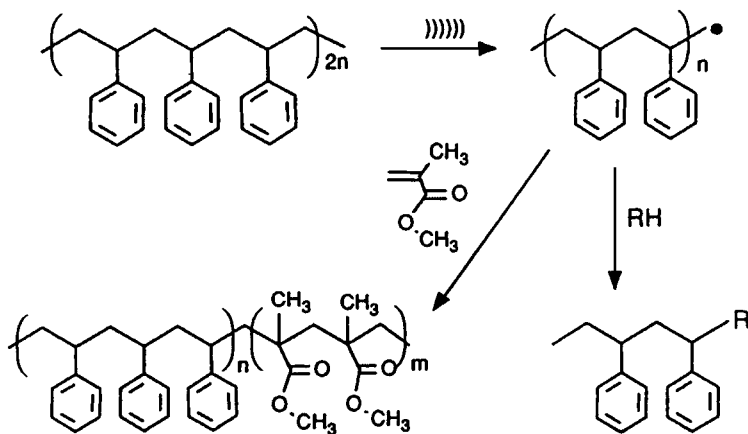
Figure 4   Sonochemical production of end-capped polymers and block copolymers (11).

controlling the block structure. An alternative approach (GJ Price, unpublished data) involves sonicating a polymer dissolved in a solution containing the second monomer. The macromolecular radical initiates polymerization of the second monomer, as illustrated in Figure 4 for polystyrene and methyl methacrylate.

By using the results of degradation studies, the structure and block length of the first polymer can be controlled quite precisely. By changing the concentration of monomer in solution, the block size of the second polymer can also be varied, allowing a large degree of control over the resulting material structure. A related approach is to sonicate the polymer in the presence of a species labile to radical attack, forming end-capped polymers. One may also use this approach to prepare, for example, polystyrene- and poly(alkane)-bearing fluorescent groups.

SONOCHEMICAL MODIFICATION OF POLYMER SURFACES   As mentioned above, bubble collapse near a surface results in jets of liquid impinging at high velocity onto the surface. These are primarily responsible for the cleaning action of ultrasound but can also be used to effect chemical change at the surface.

One of the first reports of this technique was by Urban & Salazar-Rojas (40), who worked with poly(vinylidene difluoride), a piezoelectric material. This is normally an insulator, but after treatment with a strong base, dehydrofluorination will produce a surface with carbon-carbon double bonds, and ultrasound accelerates this process significantly. The enhanced contact between the solid surface and the solution promoted by ultrasound provided excellent wetting of the surface as well as better mass transport of reagents. The unsaturated sites

can be reacted further; for example, phthalocyanine dyes (41) can be grafted onto the fluorocarbon polymer surface.

Related work has involved poly(vinyl chloride), PVC, an inexpensive, commodity polymer. Functionalizing the surface would confer the surface properties of more expensive polymers in an inexpensive manner. A number of compounds including metal ions, dyes, and hydrophilic monomers have been grafted to the surface (GJ Price, AA Clifton, unpublished data). In this way, one can change the chemical nature of the surface so that it has greater functionality than the base polymer. A more difficult example is polyethylene, which is widely used but has an inert surface that makes adhesion or printing very difficult. Current methods involve activation with chromic acid or an oxygen plasma. Using ultrasound to enhance the reaction, it was possible to rapidly modify the surface character of polyethylene (43) with milder, more environmentally friendly oxidizing agents such as potassium persulfate or hydrogen peroxide. Contact angle and spectroscopic analysis indicated that a thin layer of polar groups such as hydroxyl and carbonyl had been formed on the surface, providing for greater adhesion of surface coatings.

Effects of Ultrasound on Inorganic Materials

The use of ultrasound to accelerate chemical reactions in liquid-solid heterogeneous systems has become increasingly widespread. Sonochemical enhancement of the reactivity of reactive metals as stoichiometric reagents has become an especially routine synthetic technique for many heterogeneous organic and organometallic reactions (1–7), particularly those involving reactive metals, such as Mg, Li, or Zn. Rate enhancements of more than tenfold are common, yields are often substantially improved, and byproducts are avoided. This development originated from the early work of Renaud and the more recent breakthroughs of Luche (5). The effects are quite general and apply to reactive inorganic salts and to main group reagents as well.

Distortions of bubble collapse depend on a surface several times larger than the resonance bubble size. Thus, for ultrasonic frequencies of $\sim$20 kHz, damage associated with microjet formation cannot occur for solid particles smaller than $\sim$200 μm. This takes on a special importance for sonochemistry, since fine powders are generally preferred for use as solid reagents or catalysts.

In liquid-solid slurries, cavitation still occurs, and the bubble collapse will still launch shock waves out into the liquid. When these shock waves pass over particles in close proximity to one another, high-velocity interparticle collisions can result. If the collision is at a direct angle, metal particles can be driven together at sufficiently high speeds to induce effective melting at the point of collision (18, 19), as seen in Figure 5. From the volume of the melted region of impact, the amount of energy generated during collision is determined. From
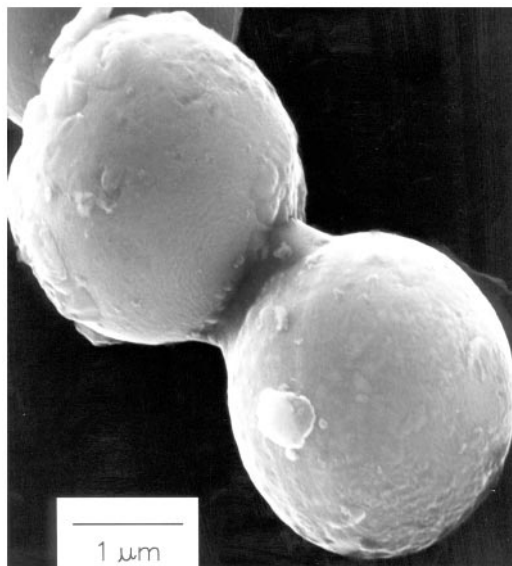
Figure 5   Scanning electron micrograph of Zn powder after ultrasonic irradiation as a slurry in decane (18).

this, a lower estimate of the velocity of impact was calculated, several hundred meters per second or roughly half the speed of sound!

If the particles collide at a glancing angle, a mechanical removal of surface material results in a macroscopic smoothing (and at the atomic level, a microscopic roughening) of the surface (as shown in Figure 6), in analogy to

Before ultrasound   **60 min. ultrasound**
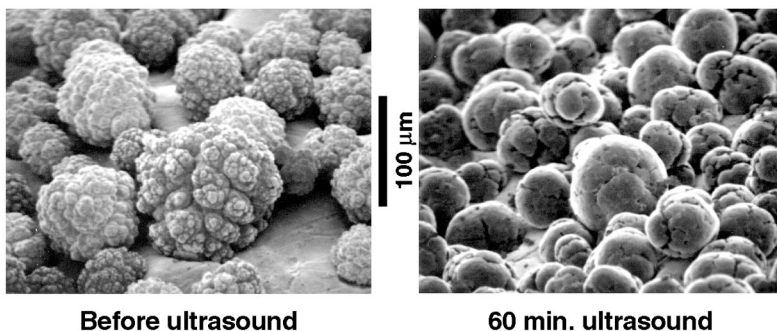
Figure 6   The effect of ultrasonic irradiation on the surface morphology of Ni powder. High-velocity interparticle collisions are created during ultrasonic irradiation of slurries (48).

lapidary ball milling. Especially for reactive metals that form oxide, nitride, or carbonaceous coatings, the consequences to the reactivity of metal particles can be quite substantial. Surface composition studies with depth profiling by Auger electron spectroscopy and by sputtered neutral mass spectrometry reveal that ultrasonic irradiation effectively removes surface oxide and other contaminating coatings (18, 44–48). The removal of such passivating coatings can dramatically improve chemical reaction rates.

To probe the conditions created during interparticle collisions in slurries irradiated with ultrasound, Doktycz & Suslick (18) examined a series of transition metal powders (Figure 7). Using the irradiation of Cr, Mo, and W powders in decane at 20 kHz and 50 W/cm^2, one observes agglomeration and what appears to be localized melting for Cr and Mo but not for W (18). A compilation of the effects of ultrasonic irradiation of slurries of different metal powders as a function of their melting points reveals a break point in aggregation and surface deformations: The effective transient temperature reached at the point of impact during interparticle collisions is roughly 3000°C. This effective local temperature has no direct connection with the temperatures inside the cavitating bubble, but they are another demonstration of the extreme conditions that ultrasound can create in an otherwise cold liquid.
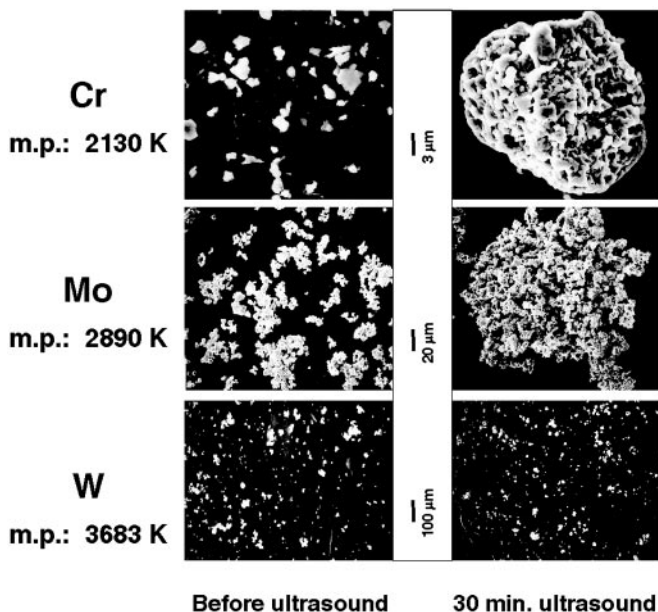

Before ultrasound   30 min. ultrasound

Figure 7   Scanning electron micrograph of Cr, Mo, and W powder after ultrasonic irradiation of decane slurries under Ar (18).

For brittle materials, most notably layered inorganic sulfides and oxides, interparticle collisions can also induce fragmentation. This can substantially increase the available surface area of the powders and thus enhance liquid-solid reaction rates. An example of this effect is found in the application of ultrasound to the process of molecular intercalation into layered inorganic solids (49, 50). The adsorption of organic or inorganic compounds between the atomic sheets of layered solids permits the systematic change of optical, electronic, and catalytic properties. Such materials have many technological applications (for example, lithium batteries, hydrodesulfurization catalysts, and solid lubricants). The kinetics of intercalation, however, are generally extremely slow, and syntheses usually require high temperatures and very long reaction times. High-intensity ultrasound dramatically increases the rates of intercalation (by as much as 200-fold) of a wide range of compounds (including amines, metallocenes, and metal sulfur clusters) into various layered inorganic solids (such as ZrS_2, V_2O_5, TaS_2, MoS_2, and MoO_3). Scanning electron microscopy of the layered solids coupled to chemical kinetics studies demonstrated that the origin of the observed rate enhancements comes from particle fragmentation (which dramatically increases surface areas) and to a lesser extent from surface damage.

Effects of Ultrasound on Heterogeneous Catalysis

Catalytic reactions are of enormous importance in both laboratory and industrial applications. Heterogeneous catalysts often require rare and expensive metals. The use of ultrasound offers some hope of activating less reactive, but also less costly, metals. Such effects can occur in three distinct stages: (*a*) during the formation of supported catalysts, (*b*) activation of preformed catalysts, or (*c*) enhancement of catalytic behavior during a catalytic reaction. As discussed below, the bulk of this research deals with the first stage, the preparation of catalysts. Some early investigations of the effects of ultrasound on heterogeneous catalysis itself can be found in the Soviet literature (12, 51). In this early work, increases in turnover rates were usually observed upon ultrasonic irradiation but were rarely more than tenfold. For modest rate increases, it appears likely that the cause is increased effective surface area; this is especially important for catalysts supported on brittle solids (e.g. noble metals supported on carbon).

More impressive effects, however, have been reported, especially for hydrogenations and hydrosilations with Ni or Raney Ni powder. For example, the hydrogenation of alkenes by Ni powder is enormously enhanced by ultrasonic irradiation (12, 44, 48). This is not caused by fragmentation of the solid; the surface area does not change significantly even after lengthy irradiation. There is, however, a very interesting effect on the surface morphology (Figure 6). Ultrasonic irradiation smoothes, at a macroscopic scale, the initially crystalline

surface and causes agglomeration of small particles. Both effects are caused by interparticle collisions owing to cavitation-induced shockwaves. Auger elemental depth profiling revealed that there is a striking decrease in the thickness of the oxide coat after ultrasonic irradiation. It is the physical removal of this passivating layer that is responsible for the $>10^5$-fold increase observed in catalytic activity.

SONOCHEMICAL PREPARATION
OF NOVEL MATERIALS

Sonochemical Synthesis of Polymers

INORGANIC-POLYMER SYSTEMS   Although not nearly as commonly used as organic materials, polymers with backbones consisting of inorganic elements have some special properties that are making them commercially significant. For example, the polysiloxanes (silicones) and polyphosphazenes remain flexible to very low temperatures. Poly(organosilanes) have a conjugated silicon backbone that confers interesting photo- and electroactive properties.

It has been reported (27) that ultrasound produces a significant acceleration in the cationic polymerization of cyclic siloxanes to give the commercially very important silicone resins. Polymers produced under sonication had narrower polydispersities but higher molecular weights than those produced under normal conditions. The acceleration of the polymerization was caused by more efficient dispersion of the acid catalyst throughout the monomer, leading to a more homogeneous reaction and hence a lower distribution of chain lengths. There is also the issue of ultrasonic degradation of long chains, which must be considered during the late stages of such polymerizations.

A second example of an inorganic polymer is also taken from silicon-based chemistry. Normally, poly(organosilanes) are prepared by a Wurtz-type coupling of dichlorodiorganosilanes that uses molten sodium in refluxing toluene to remove the halogens (52). However, yields are normally low, the reactions are difficult to reproduce, and the resulting polymers often have a very wide molecular-weight distribution and often contain two or three distinct distributions. For routine commercial use, preparation under more environmentally acceptable conditions to produce polymers with a controlled structure and preferably monomodal distribution is desirable.

The usefulness of ultrasound in this reaction was suggested by the work of Han & Boudjouk, who used lithium to couple organochlorosilanes to give R_3SiR_3 (53). Extension of the reaction by using R_2SiCl_2 gives the polymeric materials. The first reports of sonochemical synthesis of these polymers were by Kim & Matyjaszewski (54) and Kim et al (55), who produced materials

with monomodal molecular-weight distributions, albeit in rather low yield (11–15%). In contrast, Miller et al (56) reported conflicting results because sonication did not yield polymers with a monomodal distribution unless diglyme or 15-crown-5 was added to the solvent. In more recent work, Price (57) and Price & Patel (58) have established that a number of polysilanes with diverse substituents can be prepared under a range of conditions, and all give higher yields and faster reactions under ultrasound. Significantly, the effect of ultrasonic intensity on polymer molecular weights and distributions under otherwise identical conditions clearly established that higher intensities lead to narrower distributions and smaller amounts of low-molar-mass material. A similar reaction was used by Weidman and coworkers (59) to prepare polysilynes, $(RSi)_n$ with sonochemical activation of Na-K alloy. Again the use of ultrasound removed the very high-molecular-weight fractions and hence allowed the synthesis of polymers with molecular weights in the 10,000–100,000 range and monomodal distributions.

ORGANIC-POLYMER SYSTEMS   *Vinyl polymers*   The majority of organic polymers are prepared from monomers containing a reactive double bond (e.g. α-olefins and vinyl monomers), which undergo chain growth or addition reactions. These polymerize by a variety of mechanisms and, with various degrees of interest, ultrasound has been applied to examples of each type. The most straightforward preparative method is that initiated by radicals. As already noted, cavitation can produce high concentrations of radicals. Hence, application of ultrasound to vinyl monomers provides an alternative, highly controllable method of initiation.

Water itself is susceptible to cavitation and, in early work, sonochemically generated H• and OH• radicals were used by Henglein (60) to prepare poly(acrylonitrile) in aqueous solution. It was long considered that the lower degree of radical formation in organic liquids would preclude polymerization (61); this was shown to be wrong, however, and a number of workers have since studied radical polymerization both of single monomers and their mixtures.

One of the most studied systems has been methyl methacrylate. Kruus (62) and Kruus & Patraboy (62, 63) described a detailed study of the mechanism of polymerization using sonochemically generated radicals. Under some conditions, pyrolysis of the monomer occurred inside cavitation bubbles, causing the formation of significant amounts of insoluble chars in addition to linear polymers. However, as long as the monomers were properly purified and deoxygenated, soluble, high-molecular-weight polymers of methyl methacrylate and styrene could be produced. It was found that reasonable rates of conversion could be achieved over a range of temperatures and, significantly, that the reaction ceased when sonication was stopped.

The mechanistic work of Price et al (64) illustrates some of the features of sonochemical polymerization. High-molecular-weight polymers are formed early in the reaction, but the average chain length shortens at longer times. This is caused by the onset of the degradation process discussed earlier, once sufficiently long chains are formed. A conversion of $\sim$2–3% h^{-1} was achieved with methyl methacrylate at 25°C. However, above a particular conversion, the viscosity increase suppresses both cavitation and the consequent radical formation, and no further conversion to polymer occurs.

The primary role of ultrasound in this type of reaction is to produce the radicals needed to initiate polymerization. This can take place by two routes. Sonication of pure monomers produces radicals through decomposition inside the bubble or at its interface; alternatively, the decomposition of added initiators such as peroxides or azo compounds could be accelerated (64, 65). Kinetic results at 25°C indicate that sonication increased the rate of decomposition of 2,2′azobisisobutyronitrile (AIBN) over the conventional reaction by some three orders of magnitude. This may be related to thermal effects in the interfacial regions around cavitating bubbles. By suitable manipulation of conditions such as temperature, solvent vapor pressure, and ultrasonic intensity, one may predict and control the rate of initiation.

The kinetics of the other parts of the polymerization have been measured (62, 64). To summarize, the rate was found to be proportional to the monomer concentration and to depend on the square root of ultrasonic intensity. The final molecular weight varied inversely with the monomer concentration and scaled inversely with the square root of the ultrasonic intensity. By analogy with the usual treatment of radical polymerization kinetics, a detailed mechanism was proposed for the sonochemical process. Essentially, the rate of initiation is proportional to the number of cavitation sites available, which depends in turn on the ultrasound intensity. Using this mechanism, the time dependence of the rate of polymerization, the molecular weight, and the conversion to polymer were described and were in good agreement with the experimental observations.

In contrast to the initiation, higher temperatures led to an increase in the rate of polymerization. The termination steps, being bimolecular radical reactions, do not depend strongly on temperature, whereas addition of monomer to the growing chain is controlled by diffusion and thus would be expected to increase with temperature. The experimental results suggest that ultrasound has relatively little effect on the propagation or termination reactions, compared with the acceleration of initiation. This conclusion is also supported by the small amount of published work on copolymerization, in which two or more different monomers can be incorporated into the same polymer chain. If ultrasound were affecting the propagation, differences in the sequences of the two

monomers along the chain would be expected. No significant differences were found by Miyata & Nakashio (66) for styrene-acrylonitrile copolymerizations or by Price et al (67) for mixtures of styrene with methyl or butyl methacrylates.

An alternative route for vinyl polymerizations uses a latex dispersion as an emulsion or suspension in an aqueous medium. In addition to water and the monomer(s), a number of other components (such as stabilizers, dispersants, and initiators) are usually added. The large degree of motion induced by acoustic streaming and cavitation shockwaves creates very high shear forces, which act to break up droplets of liquid and maintain a small and even distribution of droplet sizes.

The first reports of applying ultrasound to this type of reaction date from the early 1950s when it was found that better dispersion of styrene was obtained under sonication (68), which also significantly accelerated the rate of polymerization. In the most recent example of this type, Cooper and coworkers (69) have used a horn system to produce latexes of polystyrene, poly(butyl acrylate) and poly(vinyl acetate) with low amounts of or even no surfactant and with smaller particle sizes than in conventional processes. The rates of reaction were also accelerated but, as expected, this depended on the vapor pressure of the monomer. In contrast to the bulk or solution polymerizations described earlier, conversions of ~100% were routinely achieved.

There has been only a small amount of work on polymerizations proceeding via an ionic mechanism. Schultz et al (70) described how sonication had little effect on the anionic polymerization of styrene itself but allowed the butyl lithium initiators to be prepared at faster rates than under conventional conditions. Additionally, successful initiators could be prepared even in undried solvents. These findings parallel much of the work in synthetic sonochemistry of organometallic compounds (5, 6, 9).

Other organic polymers   Although vinyl polymers are an important class of materials, there are a wide variety of other compounds that are polymerized by other mechanisms. Perhaps the largest group of these is the condensation or step growth polymerizations. Given the large number of industrially important polymers and plastics (e.g. polyesters, polyurethanes, and nylons) prepared by condensation reactions, there have been surprisingly few reports of the application of ultrasound in this area.

Among the very few other published studies is the patent of Long (71), who described various reactors that incorporated ultrasonically vibrating walls. These could be used for the precise control of both when and where polymerization took place for several polyurethane systems and were especially useful for producing foams. Another commercially significant mechanism for producing polymers is the ring-opening mechanism of a cyclic monomer. A

range of polyesters can be produced from cyclic lactones, but probably the most commercially significant in terms of amount of polymer manufactured is the reaction of ε-caprolactam to give nylon-6. This normally is a two-stage process where the initial ring opening is catalyzed by a small amount of water, and this is followed by polymerization to high molecular weight under vacuum. Ragaini (72a) and Carli et al (72b) showed that application of ultrasound enhanced the ring-opening phase, allowing a single-step polymerization without the need to add water to start the reaction. High-molecular-weight materials with narrower distributions were formed in shorter reaction times and at lower temperatures than with the conventional process.

The examples described thus far have dealt with linear polymers. Many items, however, are manufactured from elastomeric, lightly cross-linked materials, e.g. tubes and tires made from natural or synthetic rubber. Cross-linking is often carried out by heating with sulfur, a process known as vulcanization. Long processing times and high temperatures must be used because rubber is a poor conductor of heat, so that it is a very energy-intensive process. In the sonochemical process (73), the heat is generated inside the article from acoustic attenuation, so the reaction is faster and less thermal degradation of the rubber occurs. In some cases, both the treatment time and the energy requirements were lowered 50%. The same ultrasonic heating method can be applied to other systems such as epoxy resins (74). In a new application (75) of sonochemical technology, the opposite effect can be used, in which a combination of heat, pressure, and ultrasound breaks the cross-links, permitting the recycling of waste rubber such as car tires.

Biomaterials Preparation: Protein Microspheres

Another important application of sonochemistry to materials chemistry has been the preparation of biomaterials, most notably protein microspheres (76–82). Although the chemical effects of ultrasound on aqueous solutions have been studied for many years, the development of aqueous sonochemistry for biomaterial synthesis is very recent, particularly in the area of microencapsulation. It is beyond the scope of this chapter to review this area thoroughly, but a brief synopsis and bibliography are provided.

With high-intensity ultrasound and simple protein solutions, a remarkably easy method to make both air-filled microbubbles and nonaqueous liquid-filled microcapsules has been developed. Figure 8 shows an electron micrograph of sonochemically prepared microspheres. These microspheres are stable for months and, being slightly smaller than erythrocytes, can be intravenously injected to pass unimpeded through the circulatory system.

The mechanism responsible for microsphere formation is a combination of two acoustic phenomena, emulsification and cavitation. Ultrasonic
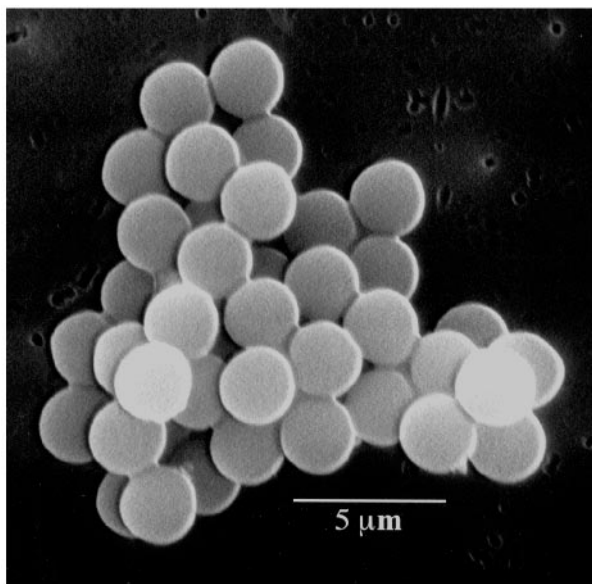
Figure 8   Scanning electron micrograph of sonochemically prepared protein microspheres from bovine serum albumin (6).

emulsification creates the microscopic dispersion of the protein solution necessary to form the proteinaceous microspheres. Alone, however, emulsification is insufficient to produce long-lived microspheres. The long life of these microspheres comes from a sonochemical cross-linking of the protein shell. Chemical reactions requiring O_2 are critical in forming the microspheres. It has been known for some time that the primary products from the sonolysis of water are H_2 and H_2O_2, yielding H• and OH•; in the presence of O_2, the latter produces HO_2 (83).   Based on chemical trapping experiments, Wong & Suslick (80) established that the proteinaceous microspheres are held together by disulfide bonds between protein cysteine residues and that superoxide is the cross-linking agent. The cross-linked shell of the microspheres is only ∼10 protein molecules thick, as shown in transmission electron micrographs of protein-stained microtome sections from sonochemically prepared protein microspheres.

These protein microspheres have a wide range of biomedical applications, including their use as echo contrast agents for sonography (84), magnetic-resonance-imaging contrast enhancement (79, 81, 82), and oxygen or drug delivery (80), among others. An extensive body of patent literature now exists in this area (85–96).

Inorganic Nanostructured Materials Synthesis

Solids made from nanometer-sized components often exhibit properties distinct from those of the bulk, in part because clusters that small have electronic structures with a high density of states yet no continuous bands (97, 98). Such nanostructured materials have been a matter of intense current interest, and several preparative methods have been developed for their synthesis. Nanostructured materials syntheses include gas-phase techniques (e.g. molten-metal evaporation and flash vacuum thermal and laser pyrolysis decomposition of volatile organometallics), liquid-phase methods (e.g. reduction of metal halides with various strong reductants and colloid techniques with controlled nucleation), and mixed-phase approaches (e.g. synthesis of conventional heterogeneous catalysts on oxide supports, metal atom vapor deposition into cryogenic liquids, and explosive-shock synthesis). To this range of techniques, over the past 10 years the sonochemical reactions of volatile organometallics have been exploited as a general approach to the synthesis of nanophase materials, as shown in Figure 9.

Using the extreme conditions inside a cavitating bubble, Suslick and coworkers have produced a variety of nanostructured and often amorphous metals, alloys, and carbides and examined their catalytic activity (99–114). Volatile
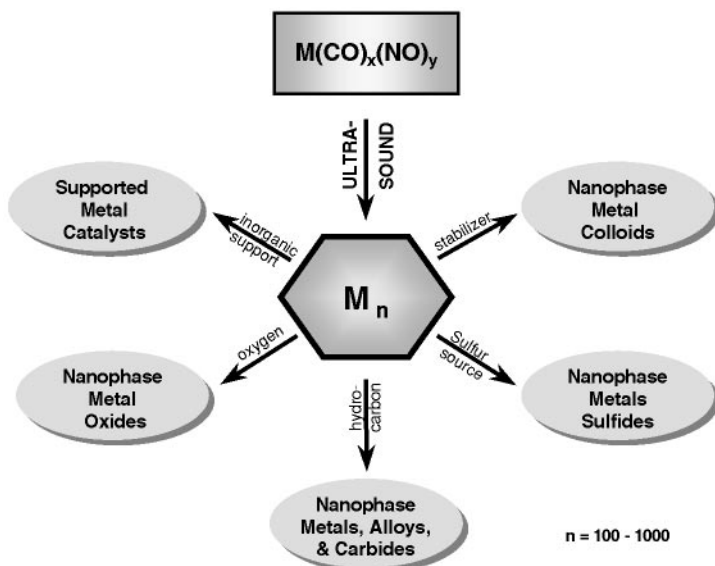

Figure 9 Sonochemical synthesis of nanostructured materials.

organometallic compounds decompose inside a collapsing bubble, and the resulting metal atoms agglomerate to form nanostructured materials. This sonochemical synthesis of nanostructured materials is extremely versatile; various forms of nanophase materials can be generated simply by changing the reaction medium. When precursors are sonicated in high-boiling-point alkanes, nanostructured metal powders are formed. If sonication occurs in the presence of a bulky or polymeric surface ligand, stable nanophase metal colloids are created. Sonication of the precursor in the presence of an inorganic support (silica or alumina) provides an alternative means of trapping the nanometer clusters. The nanoparticles trapped on these supports produce active supported heterogeneous catalysts.

AMORPHOUS METALS, ALLOYS, AND COLLOIDS   The ultrasonic irradiation of solutions containing volatile transition metal organometallic compounds [e.g. $Fe(CO)_5$, $Ni(CO)_4$, and $Co(CO)_3NO$] produces highly porous aggregates of nanometer-sized clusters of amorphous metals (99–102). For example, sonication of 1 M iron pentacarbonyl in decane at $0°C$ under argon yielded a dull black powder. Elemental analysis of the powder, after heating at $100°C$ under vacuum to remove residual solvent, showed it to be >96% iron by weight, with trace amounts of carbon (<3%) and oxygen (1%, by difference), presumably from the decomposition of alkane solvent or carbon monoxide during ultrasonic irradiation. Scanning electron micrographs revealed that the powder is an agglomerate of 20-nm particles (Figure 10). Transmission electron micrographs further indicated that these 20-nm particles consist of smaller ~4- to 6-nm particles.

The amorphous nature of the iron powder was confirmed by several different techniques, including scanning electron microscopy, differential scanning calorimetry, electron microdiffraction, powder x-ray diffraction (XRD), and neutron diffraction. Initial powder XRD showed no diffraction peak; after heat treatment under helium at $350°C$, the diffraction lines characteristic of bcc iron metal are observed. Electron microdiffraction revealed a diffuse ring pattern, characteristic of amorphous materials. Differential scanning calorimetry also showed one exothermic irreversible disorder-order transition temperature at $308°C$. The amorphous metal formation appeared to result from the extremely high cooling rate during acoustic cavitation.

There had been a long-standing controversy concerning the magnetic properties of amorphous iron, which had not been previously available without substantial amounts of added alloying elements (e.g. boron). Magnetic studies of the sonochemically prepared amorphous iron showed that amorphous iron is a very soft ferromagnetic material with a saturation magnetization density of ≈173 emu/g and a Curie temperature in excess of 580 K. The effective magnetic moment is 1.7 μ_B, with an effective exchange constant of only ≈30% of

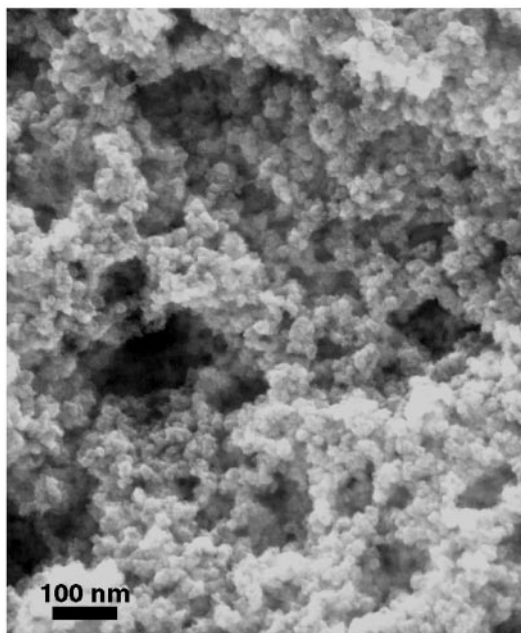*Figure 10*   Amorphous iron prepared by the sonochemical decomposition of Fe(CO)$_5$ (99).

crystalline Fe (101). The neutron diffraction data (102) confirmed these measurements and were consistent with a random packing model, as in many thin amorphous metal films. The magnetic properties fall close to those of liquid iron.

Sonochemical techniques can also be used to prepare nanostructured alloys. Suslick and coworkers (103–114) first demonstrated this for Fe-Co alloys, chosen because Fe(CO)$_5$ and Co(CO)$_3$(NO) were readily available as precursors that are thermally stable at the modest bulk solution temperatures necessary for high volatility. The composition of the Fe-Co alloys can be controlled simply by changing the ratio of solution concentrations of the precursors; alloy compositions ranging from pure Fe to pure Co are readily obtained and homogeneous on a nanometer scale (104–106). As with iron, the cobalt and Fe-Co alloys produced by ultrasound are initially amorphous, as determined by XRD and electron-beam microdiffraction. The catalytic properties of the sonochemically prepared Fe, Co, and Fe-Co alloys in the cyclohexane reaction exhibit an interesting effect: Fe-Co alloys generate much more dehydrogenation product (benzene) than pure Fe or Co owing to selective poisoning of the sites responsible for hydrogenolysis by small amounts of surface carbon. Significant recent work by Gedanken and his group have extended the sonochemical synthesis of

nanostructured alloys to Co-Ni and Fe-Ni systems (115, 116). Again the materials are amorphous as initially prepared with near uniform particles of ~6 to 10 nm. Magnetic measurements indicated that the Co-Ni alloy particles were superparamagnetic.

The existence of aggregates of nanometer clusters in our sonochemically prepared materials suggests the possibility of trapping these particles before they aggregate. Colloids of ferromagnetic materials are of special interest owing to their many important technological applications as ferrofluids (117). Such magnetic fluids find uses in information storage media, magnetic refrigeration, audio reproduction, and magnetic sealing. Commercial magnetic fluids are generally produced by exhaustive grinding of magnetite (Fe_3O_4) in ball or vibratory mills for several weeks in the presence of surfactants, which produces a very broad particle size distribution (117).

Suslick and coworkers developed a new method for the preparation of stable ferromagnetic colloids of iron using high-intensity ultrasound to sonochemically decompose volatile organometallic compounds (112). These colloids have narrow size distributions centered at a few nanometers and are found to be superparamagnetic. Sonochemical decomposition of iron pentacarbonyl in the presence of stabilizers such as poly(vinyl pyrrolidone) or oleic acid produced a colloid of nanometer-sized iron particles. Transmission electron micrographs showed that the iron particles have a relatively narrow range in size, from 3 to 8 nm for poly(vinyl pyrrolidone), whereas oleic acid gives an even more uniform distribution at 8 nm (Figure 11). Electron microdiffraction revealed that the particles are amorphous on the nanometer scale as formed and that, after in situ electron beam heating, these particles crystallize to bcc iron.

Magnetic studies indicate that these colloidal iron particles are superparamagnetic with a saturation magnetization density of a respectable 101 emu/g (Fe) at 290 K. High saturation magnetization is desirable for magnetic fluid application and is highly sensitive to the method of preparation. Bulk amorphous Fe saturates at 156 emu/g (Fe) (101, 102, 111). For a comparison, the saturation magnetization of a commercial magnetite-based magnetic fluid is 123 emu/g Fe (Ferrofluids Corp, Nashua, NH, catalog #APG-047). Kataby et al (118) found similar results with long-alkyl-chain alcohols on nanophase amorphous-Fe nanoparticles. The formation of chemical bonds between the substrate and the alcohols was demonstrated by Fourier transform infrared spectroscopy (FTIR) and x-ray photoelectron spectroscopy (XPS) measurements (118). This group has also sonochemically produced colloidal cobalt solutions in decalin stabilized by oleic acid and Fe_2O_3 colloidal solutions in hexadecane stabilized by oleic acid (119, 120).

A different approach to the sonochemical synthesis of nanostructured metals is by cavitation to produce strong reductants from aqueous or alcohol solutions, thereby reducing metal salts in situ. Several researchers have used this approach.
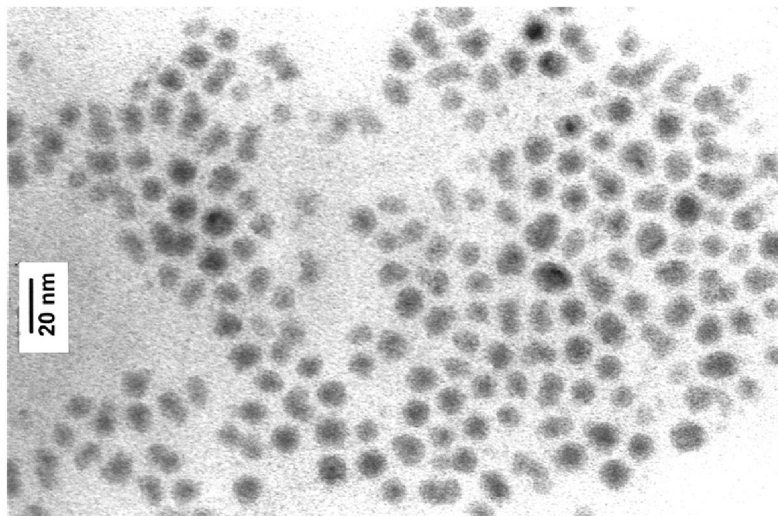
Figure 11   Transmission electron micrograph of sonochemically-prepared iron colloid stabilized by oleic acid (112).

For example, gold colloids can be produced by the sonochemical reduction of $AuCl_4^-$ solutions under Ar (121). The colloid particle sizes had number averages of about 10 nm, with a fairly narrow size distribution, and could be stabilized for months by using the usual surfactants. Grieser and coworkers found that the addition of aliphatic alcohols significantly enhanced the rate of colloid formation and that the more hydrophobic the alcohol, the greater the effect (122). They concluded that radical reductants were being generated from the alcohols in the interfacial region surrounding the cavitation bubbles. Dhas et al recently reported (123) the synthesis of metallic copper nanoparticles (porous aggregates of 50–70 nm that contain an irrregular network of small nanoparticles) from aqueous sonolysis of a copper(II) hydrazine complex.

NANOSTRUCTURED SUPPORTED CATALYSTS   Most heterogeneous metal catalysts are supported, i.e. the metal is deposited on a high-surface-area solid, such as silica or alumina. In general, these materials are made by taking simple metal salts (usually the nitrates), soaking aqueous solutions of them into the porous support, and calcining under hydrogen at high temperatures to produce small metal particles throughout the support. Often the metal particles are not very uniform in size and are dispersed throughout the ill-defined pore structure of the support. The creation of "eggshell" catalysts in which uniform-sized nanoparticles of metals are deposited on the outer surface of supports has potential advantages for catalyst preparation (124).

Suslick and coworkers found that ultrasonic irradiation of decane solutions of iron pentacarbonyl, $Fe(CO)_5$, in the presence of silica gel produces a silica-supported amorphous nanostructured iron in which the iron particles are all on the outer surface of the silica (104, 109). The iron particles are formed during cavitation events and then deposited on the silica suspended in solution. The iron loading on the SiO_2 can be easily varied by changing the initial concentration of the $Fe(CO)_5$ solution. The amorphous nature of these supported iron particles as initially deposited has been confirmed by several different techniques, which also showed crystallization to α-Fe metal particles on heating above 300°C. Transmission electron microscopy showed that the iron particles produced by sonolysis of $Fe(CO)_5$ were highly dispersed on the SiO_2 surface. The iron particles range in size from 3 to 8 nm. The particles are on the surface of the silica only, which gives a very different surface morphology to the silica compared with that of a conventionally prepared catalyst. In closely related studies, Ramesh et al prepared Fe and Fe_3O_4 particles on the surface of colloidal nonporous silica (125). In either system, high-temperature drying of the silica is necessary to prevent oxidation of the iron nanoparticles.

The catalytic activity of the silica-supported nanostructured iron was probed in the commercially important Fischer-Tropsch synthesis reaction (i.e. hydrogenation of CO) (104, 109). The major reaction products for both catalysts are short-chain C_1 to C_4 hydrocarbons and CO_2. The catalytic activity of the sonochemically produced iron on silica catalyst is an order of magnitude higher than the conventional supported iron at similar loadings and dispersions. Moreover, the silica-supported nanostructured iron catalyst exhibits high activity at low temperatures (<250°C), whereas the conventional catalyst has no activity. The dramatic difference in activity between the two samples below 300°C may be caused by the amorphous nature of iron and the inherently highly defective surface formed during sonolysis of $Fe(CO)_5$, when the amorphous state of iron is preserved. At higher temperatures, the activity decreases owing to iron crystallization, surface annealing, or catalyst deactivation from surface carbon deposition.

NANOSTRUCTURED CARBIDES, NITRIDES, OXIDES, AND SULFIDES

Carbides and Nitrides

Molybdenum and tungsten carbides have been explored as heterogeneous catalysts because of the similar activity that these carbides share with platinum group metals (126–128). For catalytic applications, high-surface-area materials are generally needed, but the refractory nature of these carbides makes this very

difficult. Suslick and coworkers (106–110) have developed a simple sonochemical synthesis of nanophase molybdenum carbide from the ultrasonic irradiation of molybdenum hexacarbonyl (106–110). Sonochemical decomposition of molybdenum hexacarbonyl in hexadecane produced an amorphous molybdenum oxycarbide; the oxygen was removed by heating under 1:1 CH_4/H_2. The elemental analytical results showed that the sample had a stoichiometry of $Mo_2C_{1.02}$ with <0.09 wt% oxygen (by difference) and <0.02 wt% hydrogen. Scanning electron microscopy showed that the surface is extremely porous, and transmission electron microscopy revealed that the material is a porous aggregate of 3-nm-diameter particles; gas adsorption showed a surface area of 130 m^2/g.

Catalytic dehydrogenation versus hydrogenolysis of cyclohexane served as a standard reaction with a flow catalytic microreactor. To compare the catalytic properties, commercial ultrafine powders of platinum and ruthenium were also used under identical conditions. At all reaction temperatures examined, benzene was the only product formed for both samples, and their activities were comparable; no hydrogenolysis products were detected. In contrast, only hydrogenolysis, mostly to methane, occurred with commercial ruthenium powder. The analogy has often been made that Mo_2C is similar to Ru, whereas W_2C behaves like Pt (129). These results demonstrate, however, that for dehydrogenation of alkanes, sonochemically prepared nanostructured molybdenum carbide has selectivity similar to Pt rather than to Ru.

There is only one report in the literature concerning the sonochemical preparation of nitrides (130). $Fe(CO)_5$ was sonicated in a decane solution under a gaseous mixture of NH_3 and H_2 at $\sim0°C$. Alternatively, the sonochemically prepared amorphous iron was nitrided at $\sim400°C$ under a mixed stream of NH_3 and H_2. Different products were obtained in the two cases. The product of the first preparation was an amorphous $Fe_{2-3}N$ and a small quantity of iron oxide (presumably from adventitious air). In the second case, the XRD patterns showed FeN as a main product.

Nanostructured Oxides

Ultrasound for the preparation of both main-group and transition metal oxides has found some significant use. For example, the ultrasonic irradiation of $Si(OC_2H_5)_4$ in water with an acid catalyst produces a silica "sonogel" (131). In conventional preparation of silica gels from $Si(OC_2H_5)_4$, ethanol is typically used as a cosolvent, because $Si(OC_2H_5)_4$ is not soluble in water. Such solvents can become problematic because they may cause cracking during drying. These volatile cosolvents become unnecessary with sonication owing to enhanced mixing. The silica sonogel produced by the sonication of $Si(OC_2H_5)_4$ in the absence of ethanol has a higher density than the conventionally prepared gel.
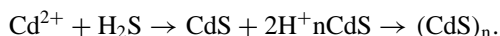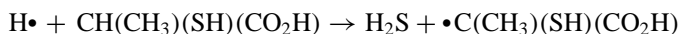
The particle size is also smaller than that of conventional gels (132). Small-angle x-ray–scattering experiments have been conducted on a silica sonogel and conventional silica aerogel. Conventional aerogels consist of a low-density matrix with large empty pores. The sonogels, in contrast, have finer porosity and the pores are approximately sphere-shaped, with a smooth surface (133). Monolithic silica glasses have been produced from silica sonogels prepared to 1150°C (134). Zirconium sonogels have also been produced from sonication of zirconium tetrapropoxide with acetic acid. Gelation time was reduced on sonication, and the sonogel had a much smaller particle size (135). Finally, this technique has been extended to trap large, organic dye molecules within the sonogel (136).

The synthesis of hydroxyapatite, $Ca_5(PO_4)_3OH$, from the hydrolysis of calcium oxyphosphates is also accelerated by ultrasound (137). Extensive research has been conducted on the synthesis of hydroxyapatite, owing to its potential application in medicine as artificial bone. The reaction time required to produce hydroxyapatite from a mixture of $Ca_4(PO_4)_2O$ and $CaHPO_4(H_2O)$ (brushite) at 38°C was reduced from 3 h without sonication to 15 min with sonication. XRD showed that neither product was very crystalline. The morphologies of these two products were, however, quite different. The hydrolysis of α-$Ca_3(PO_4)_2$ (α-TCP) produced hydroxyapatite with better crystallinity. This reaction was also accelerated by ultrasonic irradiation.

In related work, Gasgnier and coworkers reported the acceleration formation of rare earth oxide formation via ultrasound (138), and Cao et al (139), Shafi et al (140), and Kataby et al (141) have extended the sonochemical synthesis of amorphous transition metals to the production of nanostructured metal oxides, simply by sonication in the presence of air (139–141).

Sulfides

Nanocrystalline CdS colloids have been produced by high-intensity ultrasound (142), as shown in the equations below. In situ–generated hydrogen sulfide from the sonication of 2-mercaptopropionic acid acted as the sulfiding agent. Spectroscopic studies revealed that sonication produces CdS particle sizes in the quantum dot range (Q-state) and the sonication time and the thiol type determine the particle size distribution. The colloid particles produced by the ultrasound process clearly show quantum size effects and are estimated to be <3 nm in diameter.

$$H\bullet + CH(CH_3)(SH)(CO_2H) \rightarrow H_2S + \bullet C(CH_3)(SH)(CO_2H)$$

$$Cd^{2+} + H_2S \rightarrow CdS + 2H^+ nCdS \rightarrow (CdS)_n.$$

Very recently, Mdleleni et al reported the sonochemical synthesis of nano-structured molybdenum sulfide (114). MoS_2 is best known as the standard
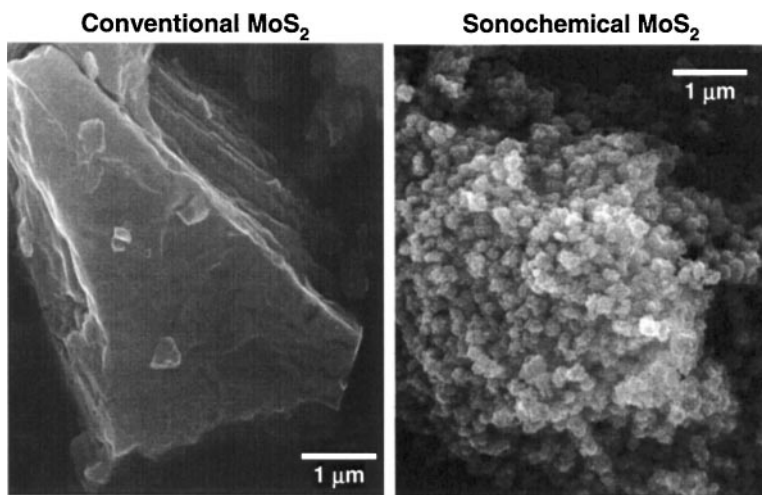
Figure 12 Morphology of conventional and sonochemically prepared MoS_2; scale bar is 1 μm (114).

automotive lubricant; its lubricant properties are caused by its layered structure. Planes of molybdenum atoms are sandwiched on both faces by planes of sulfur atoms tightly bonded to the Mo. Interactions between the sulfur planes are weak, thus producing lubrication properties similar to graphite. Of greater interest here, however, MoS_2 is also the predominant hydrodesulfurization catalyst heavily used by the petroleum industry to remove sulfur from fossil fuels before combustion (143).

An unusual morphology of MoS_2 was produced by the irradiation of solutions of molybdenum hexacarbonyl and sulfur in 1,2,3,5-tetramethylbenzene with high-intensity ultrasound (114). The morphologies of the sonochemical and conventional MoS_2 are dramatically different, as shown in Figure 12. Conventional MoS_2 shows a platelike morphology typical for such layered materials. The sonochemical MoS_2 exists as a porous agglomeration of clusters of spherical particles with an average diameter of 15 nm. Despite the morphological difference between the sonochemical and conventional MoS_2, transmission electron microscopy images (Figure 13) show both to have the same interlayer spacing. The sonochemically prepared MoS_2, however, shows much greater edge and defect content because the layers must bend, break, or otherwise distort to fit to the outer surface of the 15-nm particle size (Figure 13).

It is well established that the activity of MoS_2 is localized at the edges and not on the flat basal planes (143, 144). Unfortunately, the nature of this
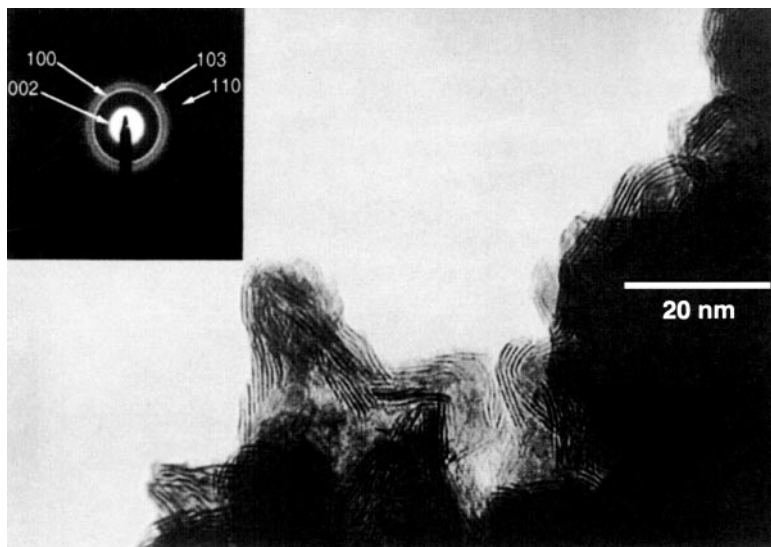
Figure 13   Transmission electron micrograph of sonochemically prepared MoS_2. Basal planes are seen as dark fringes with interlayer spacings of 0.62 ± 0.01 nm, the same as conventional MoS_2 (114).

layered material causes the basal planes to dominate the total surface area under most synthetic conditions. Given the inherently higher edge concentrations in nanostructured materials, the catalytic properties of our sonochemically prepared MoS_2 become especially interesting. The catalytic activity and selectivity for thiophene hydrodesulfurization by sonochemically prepared MoS_2 were examined in a single-pass microreactor (114). Conventional MoS_2, sonochemical Mo_2C, and commercial ReS_2 and RuS_2 were also investigated under the same conditions for comparison. For conventionally prepared sulfides, ReS_2 and RuS_2 are inherently more reactive than MoS_2 (144) but are too expensive to be generally used. The observed turnover frequencies for these catalysts were examined as a function of temperature. The principal products detected by gas chromatography were the C_4 hydrocarbons: butadiene, 1-butene, *trans*-2-butene, *cis*-2-butene, and butane. The observed order of hydrodesulfurization activity is MoS_2 (sonochemical) > RuS_2 (conventional) > ReS_2 (conventional) > Mo_2C (sonochemical) > MoS_2 (conventional). The sonochemically prepared MoS_2 catalyzes the hydrodesulfurization of thiophene with activities roughly fivefold better than conventional MoS_2 and comparable to those observed with RuS_2, one of the best commercial catalysts.

CONCLUSIONS

Bubble collapse in liquids results in an enormous concentration of energy from the conversion of the kinetic energy of liquid motion into heating of the contents of the bubble. The enormous local temperatures and pressures so created provide a unique means for fundamental studies of chemistry and physics under extreme conditions.

Cavitation in liquids can have dramatic effects on the reactivities of both extended solid surfaces and fine-powder slurries. Microjet and shockwave impact (on large surfaces) and interparticle collisions (with powders) have substantial effects on the chemical composition and physical morphology of solids that can dramatically enhance chemical reactivity of both organic polymers and inorganic solids.

The extreme conditions inside collapsing bubbles produce highly reactive species that can be used for various purposes, for instance, the initiation of polymerization without added initiators. As another example, the sonochemical decomposition of volatile organometallic precursors in high-boiling-point solvents produces nanostructured materials in various forms with high catalytic activities. Nanostructured metals, alloys, carbides and sulfides, nanometer colloids, and nanostructured supported catalysts can all be prepared by this general route.

We have seen a diverse and promising set of applications for ultrasound in materials chemistry. There still remains, however, much to explore in the sonochemical synthesis of organic, inorganic, and even biomaterials.

> **Visit the *Annual Reviews home page* at
> http://www.AnnualReviews.org**

Literature Cited

1. Suslick KS, ed. 1988. *Ultrasound: Its Chemical, Physical, and Biological Effects*. New York: VCH
2. Mason TJ, Lorimer JP. 1988. *Sonochemistry: Theory, Applications and Uses of Ultrasound in Chemistry*. Chichester, UK: Harword
3. van Eldik R, Hubbard CC, eds. 1997. *Chemistry Under Extreme or Non-Classical Conditions*. New York: Wiley & Sons
4. Suslick KS, Crum LA. 1997. In *Encyclopedia of Acoustics*, ed. MJ Crocker, 1:271–82. New York: Wiley-Interscience

5. Luche J-L. 1998. *Synthetic Organic Sonochemistry*. New York: Plenum

6. Suslick KS. 1998. In *Kirk-Othmer Encyclopedia of Chemical Technology*, 26: 517–41. New York: Wiley & Sons, 4th ed.

7. Crum LA, Mason TJ, Reisse JL, Suslick KS, eds. 1999. *Sonochemistry and Sonoluminescence, Proc. NATO Adv. Study Inst.* Ser. C Vol. 524. Dordrecht, Netherlands: Kluwer

8. Suslick KS. 1993. In *Encyclopedia of Materials Science and Engineering*, ed. RW Cahn, pp. 2093–98. Oxford, UK: Pergamon. 3rd Suppl.

9. Suslick KS. 1994. In *Encyclopedia of Inorganic Chemistry*, ed. RB King, 7:3890–905. New York: Wiley & Sons

10. Suslick KS. 1995. *MRS Bull.* 20:29

11. Price GJ. 1996. In *Chemistry Under Extreme or Non-Classical Conditions*, ed. R van Eldik, CC Hubbard. New York: Wiley & Sons

12. Suslick KS. 1997. In *Handbook of Heterogeneous Catalysis*, ed. G Ertl, H Knozinger, J Weitkamp, 3:1350–57. Weinheim: Wiley-VCH

13. Leighton TG. 1994. *The Acoustic Bubble*. London: Academic

14. Flint EB, Suslick KS. 1991. *Science* 253: 1397

15. Suslick KS, Didenko Y, Fang MM, Hyeon T, Kolbeck KJ, et al. 1999. *Philos. Trans. R. Soc. London Ser. A.* In press

16. McNamara WB III, Didenko Y, Suslick KS. 1999. In *Sonochemistry and Sonoluminescence, Proc. NATO Adv. Study Inst.* Ser. C Vol. 524. Dordrecht, Netherlands: Kluwer

17. Preece CM, Hansson IL. 1981. *Adv. Mech. Phys. Surf.* 1:199

18. Doktycz SJ, Suslick KS. 1990. *Science* 247:1067

19. Suslick KS, Doktycz SJ. 1990. In *Advances in Sonochemistry*, ed. TJ Mason, 1:197–230. Greenwich, CT: JAI

20. Mason TJ, Cordemans ED. 1996. *Chem. Eng. Res. Des.* 74:511

21. Suslick KS, Cline RE Jr, Hammerton DA. 1986. *J. Am. Chem. Soc.* 106:5641

22. Flosdorf EW, Chambers LA. 1933. *J. Am. Chem. Soc.* 55:3051

23. Gyorgi AS. 1933. *Nature* 131:278

24. Basedow AM, Ebert K. 1977. *Adv. Polym. Sci.* 22:83

25. Price GJ. 1990. See Ref. 19, pp. 231–87

26. Price GJ, Smith PF. 1993. *Eur. Polym. J.* 29:419

27. Price GJ, Wallace EN, Patel AM. 1995. In *Silicon Containing Polymers*, ed. RG Jones, p. 147. Cambridge, UK: R. Soc. Chem.

28. Koda S, Mori H, Matsumoto K, Nomura H. 1994. *Polymer* 35:30

29. Sato T, Nalepa DE. 1977. *J. Coat. Technol.* 49:45

30. Bradbury JH, O'Shea J. 1973. *Aust. J. Biol. Sci.* 26:583

31. Davison PF, Freifelder D. 1962. *Biophys. J.* 2:235

32. Encina MV, Lissi E, Sarasusa M, Gargallo L, Radic D. 1980. *J. Polym. Sci. Polym. Lett.* 18:757

33. Van der Hoff BME, Glynn PAR. 1974. *J. Macromol. Sci. Macromol. Chem.* A8:429

34. Van der Hoff BME, Gall CE. 1977. *J. Macromol. Sci. Macromol. Chem.* A11: 1739

35. Muller AJ, Odell JA, Keller A. 1990. *Macromolecules* 23:3090

36. Watanabe O, Tabata M, Kuedo T, Sohma J, Ogiwara T. 1985. *Prog. Polym. Phys. Jpn.* 28:285

37. Nguyen TQ, Liang QZ, Kausch HH. 1997. *Polymer* 38:3783

38. Deleted in proof

39. Tabata M, Miyawaza T, Sohma J, Kobayashi O. 1980. *Chem. Phys. Lett.* 73:178

40. Urban MW, Salazar-Rojas EM. 1988. *Macromolecules* 21:372

41. Exsted BJ, Urban MW. 1994. *Polymer* 35: 5560

42. Deleted in proof

43. Price GJ, Keen F, Clifton AA. 1996. *Macromolecules* 29:5664

44. Suslick KS, Casadonte DJ. 1987. *J. Am. Chem. Soc.* 109:3459

45. Suslick KS, Johnson RE. 1984. *J. Am. Chem. Soc.* 106:6856–58

46. Suslick KS, Doktycz SJ. 1989. *Chem. Mater.* 1:6

47. Suslick KS, Doktycz SJ. 1989. *J. Am. Chem. Soc.* 111:2342

48. Suslick KS, Casadonte DJ, Doktycz SJ. 1989. *Solid State Ion.* 32/33:444–52

49. Chatakondu K, Green MLH, Thompson ME, Suslick KS. 1987. *J. Chem. Soc. Chem. Commun.* 1987:900

50. Suslick KS, Casadonte DJ, Green MLH, Thompson ME. 1987. *Ultrasonics* 25:56–59

51. Mal'tsev AN. 1976. *Z. Fiz. Khim.* 50:1641

52. Miller RD, Michl J. 1989. *Chem. Rev.* 89:1359

53. Han BH, Boudjouk P. 1981. *Tetrahedron Lett.* 22:3813

54. Kim HK, Matyjaszewski K. 1989. *J. Am. Chem. Soc.* 110:3321

55. Kim HK, Uchida H, Matyjaszewski K. 1995. *Macromolecules* 28:59

56. Miller RD, Thompson D, Sooriyaku-maran R, Fickes GN. 1991. *J. Polym. Sci. Polym. Chem.* 29:813

57. Price GJ. 1992. *J. Chem. Soc. Chem. Commun.* 1992:1209

58. Price GJ, Patel AM. 1997. *Eur. Polym. J.* 33:599

59. Weidman TW, Bianconi PA, Kwock EW. 1990. *Ultrasonics* 28:310

60. Henglein A. 1954. *Makromol. Chem.* 14:15

61. El'Piner IE. 1964. *Ultrasound: Physical, Chemical and Biological Effects*. New York: Consultants Bureau

62. Kruus P, Patraboy TJ. 1985. *J. Phys. Chem.* 89:3379

63. Kruus P. 1991. *Adv. Sonochem.* 2:1

64. Price GJ, Norris DJ, West PJ. 1992. *Macromolecules* 25:6447

65. Lorimer JP, Mason TJ, Kershaw D. 1991. *J. Chem. Soc. Chem. Commun.* 1991:1217

66. Miyata T, Nakashio F. 1975. *J. Chem. Eng. Jpn.* 8:469

67. Price GJ, Daw MR, Newcombe NJ, Smith PF. 1990. *Br. Polym. J.* 23:63

68. Ostroski AS, Stanbaugh RB. 1950. *J. Appl. Phys.* 21:478

69. Cooper G, Greiser F, Biggs S. 1994. *J. Coll. Interface Sci.* 184:52

70. Schultz DN, Sissano JA, Costello CA. 1994. *Polym. Prep.* 35:514

71. Long GB. 1967. *U.S. Patent No. 3346472*

72a. Ragaini V. *Italian Patent Appl. 20478-A/90.*

72b. Carli R, Bianchi CL, Gariboldi P, Ragaini V. 1993. *Proc. Europ. Sonochem. Soc., 3rd, Coimbra, Portugal.* Eur. Sonochem. Soc.

73. Senapati N, Mangaraj D. 1985. *U.S. Patent No. 45489771*

74. Salensa TK, Babbar NK. 1971. *Ultrasonics* 13:21

75. Isayev I, Yushanov SP, Chen J. 1996. *J. Appl. Polym. Sci.* 59:803, 815

76. Suslick KS, Grinstaff MW. 1990. *J. Am. Chem. Soc.* 112:7807

77. Suslick KS, Grinstaff MW. 1991. *Proc. Natl. Acad. Sci. USA* 88:7708–10

78. Suslick KS, Grinstaff MW, Kolbeck KJ, Wong M. 1994. *Ultrason. Sonochem.* 1: S65–68

79. Liu KJ, Grinstaff MW, Jiang J, Suslick KS, Swartz HM, Wang W. 1994. *Biophys. J.* 67:896–901

80. Wong M, Suslick KS. 1995. *Hollow and Solid Spheres and Microspheres, MRS Symp. Proc.*, ed. DL Wilcox, M Berg, T Bernat, D Kellerman, JK Corchran, 372: 89–94. Pittsburgh: Mater. Res. Soc.

81. Eckburg JJ, Chato JC, Liu KJ, Grinstaff MW, Swartz HM, et al. 1996. *J. Biomech. Eng.* 118:193–200

82. Webb AG, Wong M, Kolbeck KJ, Magin RL, Wilmes LJ, Suslick KS. 1996. *J. Magn. Reson. Imaging* 6:675–83

83. Riesz P, Berdahl D, Christman CL. 1985. *Environ. Health Perspect.* 64:233

84. Keller MW, Feinstein SB. 1988. In *Echocardiography in Coronary Artery Disease*, ed. RE Kerber. New York: Future

85. Desai NP, Soon-Shiong P, Sandford PA, Grinstaff MW, Suslick KS. 1994. *U.S. Patent No. 5362478*

86. Desai NP, Soon-Shiong P, Sandford PA, Grinstaff MW, Suslick KS. 1995. *U.S. Patent No. 543686*

87. Grinstaff MW, Soon-Shiong P, Wong M, Sandford PA, Suslick KS, Desai NP. 1996. *U.S. Patent No. 5498421*

88. Grinstaff MW, Desai NP, Suslick KS, Soon-Shiong P, Sandford PA, Merideth NR. 1996. *U.S. Patent 5505932*

89. Grinstaff MW, Desai NP, Suslick KS, Soon-Shiong P, Sandford PA, Merideth NR. 1996. *U.S. Patent No. 5508021*

90. Grinstaff MW, Desai NP, Suslick KS, Soon-Shiong P, Sandford PA, Merideth NR. 1996. *U.S. Patent No. 5512268*

91. Desai NP, Soon-Shiong P, Sandford PA, Grinstaff MW, Suslick KS. 1996. *U.S. Patent No. 5560933*

92. Grinstaff MW, Soon-Shiong P, Wong M, Sandford PA, Suslick KS, Desai NP. 1997. *U.S. Patent No. 5635207*

93. Grinstaff MW, Soon-Shiong P, Wong M, Sandford PA, Suslick KS, Desai NP. 1997. *U.S. Patent No. 5639473*

94. Grinstaff MW, Soon-Shiong P, Wong M, Sandford PA, Suslick KS, Desai NP. 1997. *U.S. Patent No. 5650156*

95. Grinstaff MW, Soon-Shiong P, Wong M, Sandford PA, Suslick KS, Desai NP. 1997. *U.S. Patent No. 5665382*

96. Grinstaff MW, Soon-Shiong P, Wong M, Sandford PA, Suslick KS, Desai NP. 1997. *U.S. Patent No. 5665383*

97. Weller H. 1993. *Adv. Mater.* 5:88

98. Moser WR, ed. 1996. *Advanced Catalysts and Nanostructured Materials*. New York: Academic

99. Suslick KS, Choe SB, Cichowlas AA, Grinstaff MW. 1991. *Nature* 353:414

100. Grinstaff MW, Cichowlas AA, Choe SB, Suslick KS. 1992. *Ultrasonics* 30: 168

101. Grinstaff MW, Salamon MB, Suslick KS. 1993. *Phys. Rev. B* 48:269

102. Bellissent R, Galli G, Grinstaff MW, Migliardo P, Suslick KS. 1993. *Phys. Rev. B* 48:15797–800

103. Suslick KS, Hyeon T, Fang M, Cichowlas AA. 1994. *Molecularly Designed Nanostructured Materials, MRS Symp. Proc.,* ed. KE Gonsalves, GM Chow, TO Xiao, RC Cammarata, 351:201–06. Pittsburgh: Mater. Res. Soc.

104. Suslick KS, Fang M, Hyeon T, Cichowlas AA. 1994. *Molecularly Designed Nanostructured Materials, MRS Symp. Proc.,* ed. KE Gonsalves, GM Chow, TO Xiao, RC Cammarata, 351:443–48. Pittsburgh: Mater. Res. Soc.

105. Bellissent R, Galli G, Hyeon T, Magazu S, Majolino D, et al. 1995. *Phys. Scripta* T57:79–83

106. Hyeon T, Fang M, Cichowlas AA, Suslick KS. 1995. *Mater. Sci. Eng. A* 204:186–92

107. Suslick KS, Hyeon T, Fang M, Ries JT, Cichowlas AA. 1996. *Mater. Sci. Forum* 225–27:903–12

108. Hyeon T, Fang M, Suslick KS. 1996. *J. Am. Chem. Soc.* 118:5492–93

109. Suslick KS, Hyeon T, Fang M, Cichowlas AA. 1996. In *Advanced Catalysts and Nanostructured Materials,* ed. WR Moser, pp. 197–211. New York: Academic

110. Suslick KS, Hyeon T, Fang M. 1996. *Chem. Mater.* 8:2172–79

111. Bellissent R, Galli G, Hyeon T, Migliardo P, Parette P, Suslick KS. 1996. *J. Non-Cryst. Solids* 205:656–59

112. Suslick KS, Fang M, Hyeon T. 1996. *J. Am. Chem. Soc.* 118:11960–61

113. Long GJ, Hautot D, Pankhurst QA, Vandormael D, Grandjean F, et al. 1998. *Phys. Rev. B* 57:10716–22

114. Mdleleni MM, Hyeon T, Suslick KS. 1998. *J. Am. Chem. Soc.* 120:6189–90

115. Shafi KVPM, Gedanken A, Prozorov R. 1998. *J. Mater. Chem.* 83:769–73

116. Shafi KVPM, Gedanken A, Goldfarb RB, Felner I. 1997. *J. Appl. Phys.* 81:6901–5

117. Berkovsky BM, Medvedev VF, Krakov MS. 1993. *Magnetic Fluids: Engineering Applications.* London/New York: Oxford Univ. Press

118. Kataby G, Ulman A, Prozorov R, Gedanken A. 1998. *Langmuir* 147:1512–15

119. Shafi KVPM, Wizel S, Prozorov T, Gedanken A. 1998. *Thin Solid Films* 31:38–41

120. Shafi KVPM, Gedanken A, Prozorov R. 1998. *Adv. Mater.* 10:590–91

121. Nagata Y, Mizukoshi Y, Okitsu K, Maeda Y. 1996. *Radiat. Res.* 146:333–38

122. Grieser F, Hobson R, Sostaric J, Mulvaney P. 1996. *Ultrasonics* 34:547–50

123. Dhas NA, Raj CP, Gedanken A. 1998. *Chem. Mater.* 10:1446–52

124. Klabunde KJ, Li Y-X. 1993. *Selectivity in Catalysis,* ed. ME Davis, SL Suib, pp. 88–108. Washington, DC: Am. Chem. Soc.

125. Ramesh S, Prozorov R, Gedanken A. 1997. *Chem. Mater.* 9:2996–3004

126. Ranhotra GS, Haddix GW, Bell AT, Reimer JA. 1987. *J. Catal.* 108:40

127. Lee JS, Oyama ST, Boudart M. 1990. *J. Catal.* 125:157

128. Ledoux MJ, Pham-Huu C, Guille J, Dunlop H. 1992. *J. Catal.* 134:383

129. Volpe L, Boudart M. 1985. *J. Solid State Chem.* 59:332

130. Koltypin Y, Cao X, Prozorov R, Balogh J, Kaptas D, Gedanken A. 1997. *J. Mater. Chem.* 7:2453–56

131. Esquivias L, Zarzycki J. 1986. In *Current Topics on Non-Crystalline Solids,* ed. M Baro, DN Clavaguera, p. 409. Singapore: World Sci.

132. Esquivias L, Zarzycki J. 1988. In *Ultrastructure Processing of Advanced Ceramics,* ed. JD Mackenzie, DR Ulrich, p. 255. New York: Wiley & Sons

133. De la Rosa-Fox N, Esquivias L, Craievich AF, Zarzycki J. 1990. *J. Non-Cryst. Solids* 121:211

134. Blanco E, Ramirezdelsolar M, De la Rosa-Fox N, Esquivias L. 1995. *Mater. Lett.* 225–226:265–70

135. Chaumont D, Craievich A, Zarzycki J. 1992. *J. Non-Cryst. Solids* 147–148:41

136. Litran R, Blanco E, Ramirezdelsolar M, Esquivias L. 1997. *J. Sol-Gel Sci. Technol.* 8:985–90

137. Fang Y, Agrawal DK, Roy DM, Roy R, Brown PW. 1992. *J. Mater. Res.* 7:2294

138. Gasgnier M, Albert L, Derouet J, Beaury L. 1995. *J. Solid State Chem.* 115:532

139. Cao X, Prozorov R, Koltypin Y, Kataby G, Felner I, Gedanken A. 1997. *J. Mater. Res.* 12:402–6

140. Shafi KVPM, Koltypin Y, Gedanken A, Prozorov R, Balogh J, et al. 1997. *J. Phys. Chem. B.* 101:6409–14

141. Kataby G, Prozorov T, Koltypin Y, Cohen H, Sukenik CN, et al. 1997. *Langmuir* 13:6151–58

142. Sostaric JZ, Carusohobson RA, Mulvaney P, Grieser F. 1997. *J. Chem. Soc. Faraday Trans.* pp. 1791–95

143. Gates BC. 1992. *Catalytic Chemistry,* pp. 387–92. New York: Wiley & Sons

144. Pecoraro TA, Chianelli RR. 1981. *J. Catal.* 67:430